APPLIED AND ENVIRONMENTAL MICROBIOLOGY, Jan. 2006, p. 702–712 Vol. 72, No. 1
0099-2240/06/$08.00+0 doi:10.1128/AEM.72.1.702–712.2006

Diverse AvrPtoB Homologs from Several *Pseudomonas syringae* Pathovars Elicit Pto-Dependent Resistance and Have Similar Virulence Activities

Nai-Chun Lin,[1,2] Robert B. Abramovitch,[1,2] Young Jin Kim,[1,3] and Gregory B. Martin[1,2]*

Boyce Thompson Institute for Plant Research, Tower Rd., Ithaca, New York 14853-1801[1]; Department of Plant Pathology, Cornell University, Ithaca, New York 14853-4203[2]; and Division of Life Science and Graduate School of Biotechnology, Korea University, Seoul 136-701, South Korea[3]

Received 16 May 2005/Accepted 24 October 2005

AvrPtoB is a type III effector protein from *Pseudomonas syringae* pv. tomato that physically interacts with the tomato Pto kinase and, depending on the host genotype, either elicits or suppresses programmed cell death associated with plant immunity. We reported previously that *avrPtoB*-related sequences are present in diverse gram-negative phytopathogenic bacteria. Here we describe characterization of *avrPtoB* homologs from *P. syringae* pv. tomato T1, PT23, and JL1065, *P. syringae* pv. syringae B728a, and *P. syringae* pv. maculicola ES4326. The *avrPtoB* homolog from *P. syringae* pv. maculicola, *hopPmaL*, was identified previously. The four new genes identified in this study are designated $avrPtoB_{T1}$, $avrPtoB_{PT23}$, $avrPtoB_{JL1065}$, and $avrPtoB_{B728a}$. The AvrPtoB homologs exhibit 52 to 66% amino acid identity with AvrPtoB. Transcripts of each of the *avrPtoB* homologs were detected in the *Pseudomonas* strains from which they were isolated. Proteins encoded by the homologs were detected in all strains except *P. syringae* pv. tomato T1, suggesting that T1 suppresses accumulation of $AvrPtoB_{T1}$. All of the homologs interacted with the Pto kinase in a yeast two-hybrid system and elicited a *Pto*-dependent defense response when they were delivered into leaf cells by DC3000Δ*avrPto*Δ*avrPtoB*, a *P. syringae* pv. tomato strain with a deletion of both *avrPto* and *avrPtoB*. Like AvrPtoB, all of the homologs enhanced the ability of DC3000Δ*avrPto*Δ*avrPtoB* to form lesions on leaves of two susceptible tomato lines. With the exception of HopPmaL which lacks the C-terminal domain, all AvrPtoB homologs suppressed programmed cell death elicited by the AvrPto-Pto interaction in an *Agrobacterium*-mediated transient assay. Thus, despite their divergent sequences, AvrPtoB homologs from diverse *P. syringae* pathovars have conserved avirulence and virulence activities similar to AvrPtoB activity.

Pseudomonas syringae infects a broad range of plant species and causes significant economic losses worldwide. Over 50 pathovars of *P. syringae* have been identified based largely on their host ranges. Among these pathovars, *P. syringae* pv. tomato, the causal agent of bacterial speck disease in tomato and a pathogen of *Arabidopsis thaliana*, has been established as a model system to study plant-pathogen interactions because of its economic importance and tractability in the laboratory. Genetic analyses of the tomato-*Pseudomonas* pathosystem have revealed that resistance to *P. syringae* pv. tomato race 0 strains is specified by a pathogen avirulence gene, *avrPto*, and a single resistance gene in tomato, *Pto* (33). However, disruption of the *avrPto* gene in *P. syringae* pv. tomato strain DC3000 or JL1065 does not eliminate the ability of the mutant pathogens to elicit *Pto*-specific plant resistance (34), suggesting that there is a second *avr* gene that is recognized by Pto. Indeed, using a cross-kingdom yeast two-hybrid screening method, a second *avr* gene, *avrPtoB*, was discovered in DC3000 (23). Mutation of either *avrPto* or *avrPtoB* individually did not abolish the ability of DC3000 to elicit Pto-dependent resistance, which suggested that *avrPto* and *avrPtoB* have redundant avirulence activities (23, 34).

Although AvrPto and AvrPtoB (also known as HopAB2 [27]) exhibit limited amino acid sequence similarity, they both interact with Pto in a yeast two-hybrid system and elicit Pto-mediated cell death in tomato when they are expressed via an *Agrobacterium tumefaciens* transient assay (33). An *avrPto*/*avrPtoB* deletion mutant of DC3000 causes disease on *Pto*-expressing tomato leaves, indicating that *avrPto* and *avrPtoB* have redundant avirulence activities and are the only two avirulence genes in DC3000 that are recognized by Pto. Moreover, deletion of either *avrPto* or *avrPtoB* from DC3000 results in a subtle decrease in bacterial virulence, whereas deletion of both *avrPto* and *avrPtoB* significantly reduces the disease-forming ability of this strain (26). These data demonstrate that these two genes contribute additively to the virulence of DC3000 by promoting lesion formation in susceptible tomato plants.

AvrPto and AvrPtoB have both distinct and common virulence functions that block plant defense responses and target pathways involved in symptom development. For example, it has been reported that AvrPto can act as a suppressor of cell wall-based plant defense in *A. thaliana* (15) and that AvrPtoB enhances host susceptibility by inhibition of programmed cell death (PCD) (1, 2, 20). Recently, by using cDNA microarray analysis, a set of tomato genes involved in ethylene biosynthesis (*LeACO1* and *LeACO2*, encoding the ethylene-forming enzyme 1-aminocyclopropane-1-carboxylate oxidase) were found to be up-regulated in response to either AvrPto or AvrPtoB (7). In addition, tomato lines that are deficient in ethylene formation or perception showed markedly decreased symp-

* Corresponding author. Mailing address: Boyce Thompson Institute for Plant Research, Tower Rd., Ithaca, NY 14853-1801. Phone: (607) 254-1208. Fax: (607) 255-6695. E-mail: gbm7@cornell.edu.

TABLE 1. Bacterial strains and plasmids used for DNA manipulation

Designation	Relevant characteristics[a]	Source or reference
Strains		
Escherichia coli DH5α		Invitrogen
Escherichia coli TOP10		Invitrogen
Pseudomonas syringae pv. tomato DC3000Δ*avrPto*Δ*avrPtoB*	Δ*avrPto*::ΩSp/Sm^r, Δ*avrPtoB*::*nptII*, Rif^r Sp^r Kan^r	26
DC3000Δ*avrPto*Δ*avrPtoB*(*avrPtoB*)	DC3000Δ*avrPto*Δ*avrPtoB* containing broad-host-vector pCPP45 expressing *avrPtoB* under native *hrp* promoter, Rif^r Sp^r Kan^r Tet^r	26
T1(*avrPto*)	Broad-host-range vector pDSK519 carrying *avrPto* under native *hrp* promoter	39
Agrobacterium tumefaciens GV2260	Rif^r	30
pBTEX::*Pto*	pBTEX expressing *Pto* under the control of CaMV 35S promoter, Rif^r Kan^r	39
pBTEX::*avrPto*	pBTEX expressing *avrPto* under the control of CaMV 35S promoter, Rif^r Kan^r	39
pBTEX::*avrPtoB*	pBTEX expressing *avrPtoB* under the control of CaMV 35S promoter, Rif^r Kan^r	23
Plasmids		
pBluescript II SK(−)		Stratagene
pCR2.1	TA cloning vector, Amp^r	Invitrogen
pCPP45	Broad-host-range vector with RP4 *par* region, Tc^r	D. W. Bauer (Cornell University)
pBTEX	Derivative of binary vector pBI121 containing polylinker site between cauliflower mosaic virus 35S promoter and Nos terminator, Kan^r	R. A. Bressan (Purdue University)
pCPP2318	Broad-host-range vector carrying β-lactamase gene, Tc^r	6a

[a] Amp, ampicillin; Kan, kanamycin; Tc, tetracycline; Sp, spectinomycin; Sm, streptomycin; Rif, rifampin.

toms of bacterial speck disease. Thus, AvrPto and AvrPtoB appear to promote disease symptoms, at least in part, by up-regulating the production of ethylene in tomato leaves (7).

avrPtoB-related genes are present in diverse phytopathogenic gram-negative bacteria (19, 23). AvrPtoB exhibits 52% amino acid sequence identity with VirPphA, the first virulence effector cloned from *P. syringae* pv. phaseolicola. Ectopic expression of *avrPtoB*, *virPphA*, or the homologs $virPphA_{Pgy}$ and $virPphA_{Psv}$ restored the water-soaking ability of a plasmid-cured, nonpathogenic strain of *P. syringae* pv. phaseolicola (RW60) on bean pods, demonstrating that these genes contribute to pathogen virulence (19, 23).

Here we addressed the question of whether homologs of AvrPtoB present in diverse *Pseudomonas* pathovars have biological activity similar to that of AvrPtoB. We characterized five *avrPtoB* homologs cloned from three different *P. syringae* pathovars, *P. syringae* pv. tomato, *P. syringae* pv. syringae, and *P. syringae* pv. maculicola, which cause bacterial speck on tomato, brown spot on snap bean (*Phaseolus vulgaris* L.), and bacterial leaf spot on *Brassica* spp., respectively. We then examined the effects of ectopic expression of each of the *avrPtoB* homologs in DC3000Δ*avrPto*Δ*avrPtoB* (referred to below as Δ*avrPto*Δ*avrPtoB*) in susceptible tomato lines, as well as their ability to elicit plant resistance in tomato plants expressing Pto.

MATERIALS AND METHODS

Bacterial strains, plasmids, and DNA manipulation. The bacterial strains and plasmids used in this study are listed in Table 1. All *P. syringae* strains were grown in King's B (KB) medium (24) at 30°C unless indicated otherwise. *Escherichia coli* DH5α and TOP10 (Invitrogen, Carlsbad, CA) were used for plasmid maintenance and were grown in LB medium (13) at 37°C. *A. tumefaciens* GV2260 (30) was grown in LB medium at 30°C. The concentrations of antibiotics used in the selective media were as follows: ampicillin, 100 μg/ml; kanamycin, 50 μg/ml; rifampin, 100 μg/ml; spectinomycin, 50 μg/ml; streptomycin, 50 μg/ml; and tetracycline, 10 μg/ml.

DNA manipulation and PCR were performed using standard protocols (36). Primers used in this study are listed in Table 2. DNA and amino acid sequence analyses were performed using the DNASTAR software package (Madison, WI), and ClustalW was used for multiple-sequence alignment for AvrPtoB and AvrPtoB homologs (40). A neighbor-joining tree of AvrPtoB with nine other members of the AvrPtoB/VirPphA family was constructed using MEGA, version 2.1 (25).

Cloning of *avrPtoB* homologs. Primers avrPto2-30 and avrPto2-3 generated from nucleotide sequences of *avrPtoB* and *virPphA* were used to PCR amplify the open reading frames of *avrPtoB* homologs in *P. syringae* pv. tomato T1, PT23, and JL1065 using Turbo *Pfu* polymerase (Stratagene, La Jolla, CA). Amplified fragments were cloned into pCR2.1 for sequencing. Two or three clones of each homolog were sequenced from independent PCRs to verify there were no PCR-induced errors. The sequences obtained were then used to design internal primers for sequencing the upstream and downstream regions of each *avrPtoB* homolog using genomic DNA as the template. The sequence of the *avrPtoB* homolog in *P. syringae* pv. syringae B728a was retrieved from a draft sequence of the *P. syringae* pv. syringae B728a genome available at www.jgi.doe.gov. The *hopPmaL* sequence was retrieved from the NCBI GenBank database (accession no. AF458050). Primer sets were designed using sequences retrieved from the GenBank database to amplify the two homologs from the genomic DNA of *P. syringae* pv. syringae B728a and *P. syringae* pv. maculicola ES4326.

Preparation of bacterial cells and supernatant for RNA and protein assays. Bacteria grown overnight in 25 ml of KB medium at 30°C were washed twice with *hrp*-inducing minimal medium (HrpMM) (17) and resuspended in HrpMM. Each bacterial suspension was diluted to an optical density at 600 nm (OD_{600}) of 0.15 to 0.2 in 100 ml of HrpMM and grown at 18°C until the OD_{600} was 0.4 to 0.5. Separation of bacterial cultures into cell and supernatant fractions was performed using the protocol described previously (12). Cell pellets from each bacterial strain were separated into two parts. One part was concentrated 100-fold and 10 μl was used for protein assays, and the other part was precipitated and resuspended in 200 μl RNA*protect* bacterial reagent (QIAGEN, Valencia, CA) for RNA isolation. The supernatant proteins were precipitated with 20% trichloroacetic acid, dissolved in 20 μl 1× sodium dodecyl sulfate (SDS) sample buffer, and boiled at 100°C.

Reverse transcriptase PCR (RT-PCR). Total bacterial RNA was isolated using an RNeasy mini kit and an RNase-free DNase set (QIAGEN, Valencia, CA).

TABLE 2. Primers used to amplify *avrPtoB* homologs in different assays

Primer	Sequence (5′→3′)	Nucleotide position[a]
avrPto2-30	ATGGCGGGTATCAA(C/T)(A/G)GAGC(A/G)G	1–22
avrPto2-3	GACCTTCGAAGTGGCAGTGA	
avrPtoB-*hrp*	GGTGTGATGGAACTCTTTCCTGCTC[b]	
avrPtoBseq-1	TATCGTTCAGCAATTGGTCAGTG	393–415
avrPtoBseq-2	CCCCGGGTTCAGGTTAA	1230–1224
avrPtoBH-F	ATGGCGGGTATCAATAGAGCGG	1–22
avrPtoBH-R	TCAGGGGACTATTCTAAAAGC	1740–1720
avrPtoBHRT-F	GCCACGCGATAGCTCTTCCTTCTC	509–532
avrPtoBHRT-R	AACAACCGCCTGCCGCTCGTAAC	1377–1355
B728a-*hrp*	ACGCATCAGTGGAACCTTT[b]	
B728a-F	ATGTCGGGTATCAACGGAGCAG	1–22
B728a-R	TCAGTCAGGAACGACTCTAAAG	1551–1530
B728aseq-1	ATGCCTCAGAAATGTAATGGATAA	452–464
B728aseq-2	CTCCGCTTCAGGGTTCAG	1214–1241
hopPmaL-*hrp*	GATTTGCCGGGAGAAGTAAGG[c]	
hopPmaL-F	ATGGTAGGGATCAGTGGTAGAGCAG	1–25
hopPmaL-R	TCAAAATGCCTATGCATCAAGCC	1158–1145
hopPmaL-RT-R	GGCGAACCGGCCTAATAAT	1029–1011
16SrRNA-F	GCGGCAGGCCTAACACAT	
16SrRNA-R	GTTCCCCTACGGCTACCTT	
GWApBF	GGGGACAAGTTTGTACAAAAAAGCAGGCTTTGAGAATCTTTATTTTCAGGGCAT GGCGGGTATCAATAGAGC	
GWApBR	GGGGACCACTTTGTACAAGAAAGCTGGGTTTCAGGGGACTATTCTAAAAGC	

[a] Nucleotide position of *avrPtoB* or *avrPtoB* homolog.
[b] The *hrp* box is underlined.
[c] Upstream of *hrp* box.

One microgram of total RNA from each sample was used for first-strand cDNA synthesis with random primers and SuperScript II RNase H$^-$ reverse transcriptase (Invitrogen, Carlsbad, CA). PCR was performed using the following gene-specific primers listed in Table 2: for *avrPtoB*, avrPtoBseq-1 and avrPtoBseq-2; for $avrPtoB_{T1}$, $avrPtoB_{PT23}$, and $avrPtoB_{JL1065}$, avrPtoBHRT-F and avrPtoBHRT-R; for $avrPtoB_{B728a}$, B728aseq-1 and B728aseq-2; and for *hopPmaL*, hopPmaL-F and hopPmaL-RT-R. Primers 16SrRNA-F and 16SrRNA-R were used for amplification of 16S rRNA as an internal control.

Generation of AvrPtoB antibody. Recombinant AvrPtoB was expressed as an N-terminal glutathione *S*-transferase fusion with a tobacco etch virus (TEV) protease cleavage site directly upstream of the AvrPtoB start codon. The expression construct was generated by Gateway cloning the *avrPtoB* gene into the pDEST15 expression vector (Invitrogen, Carlsbad, CA) by following the manufacturer's protocol. Gateway-compatible *avrPtoB* was generated by PCR using the GWApBF and GWApBR primers. pDEST15::AvrPtoB was expressed in *Escherichia coli* BL21 Star(DE3) (Invitrogen, Carlsbad, CA) and was purified using standard protein expression methods (14). Briefly, glutathione *S*-transferase–AvrPtoB was purified on a column containing glutathione Sepharose 4 fast flow resin (Amersham-Pharmacia, Piscataway, NJ). The protein was cleaved from the column using 100 U of TEV protease (Invitrogen, Carlsbad, CA) and incubating the sample overnight at 4°C with gentle shaking. The cleaved protein was boiled in SDS sample buffer, separated by SDS-polyacrylamide gel electrophoresis, and stained with Coomassie blue, and AvrPtoB was excised from the gel. Polyclonal AvrPtoB antibody was generated in rabbits by Covance Research Products Inc. (Denver, PA) using acrylamide gel slices containing 2 mg of denatured AvrPtoB protein. Polyclonal AvrPtoB antiserum was affinity purified from the crude antiserum using recombinant AvrPtoB electrophoretically transferred onto polyvinylidene difluoride membranes (31).

Immunoblot assay. Protein samples from cell and supernatant fractions were electrophoresed on 8% denaturing SDS–polyacrylamide gels and electrotransferred to polyvinylidene difluoride membranes (Immobilon R; Millipore, Bedford, MA) according to the manufacturer's protocol (Bio-Rad, Hercules, CA). AvrPtoB and AvrPtoB homolog proteins were detected with ECL Plus Western blotting detection reagents (Amersham-Pharmacia, Piscataway, NJ) using purified anti-AvrPtoB primary antibodies and horseradish peroxidase-conjugated anti-rabbit immunoglobulin G secondary antibody (Promega Co., Madison, WI). Broad-host-range vector pCPP2318, which carries a constitutively expressed β-lactamase gene, was introduced into each *Pseudomonas* strain tested, and β-lactamase was used as the cytoplasmic marker. AvrPto and β-lactamase were detected using anti-AvrPto and anti-β-lactamase antibodies, respectively. Hemagglutinin (HA)-tagged AvrPtoB was detected using anti-HA primary antibodies (Roche Applied Science, Indianapolis, IN) and peroxidase-conjugated anti-rat immunoglobulin G antibody (Roche Applied Science, Indianapolis, IN).

Yeast two-hybrid interactions. A LexA yeast two-hybrid system was used to test the interaction between Pto and AvrPtoB homologs. Bait construct pEG202::Pto and prey constructs pJG4-5::AvrPto and pJG4-5::AvrPtoB were generated in previous studies (23, 39). *avrPtoB* homologs were PCR amplified using the following primer sets (Table 2): for $avrPtoB_{T1}$ and $avrPtoB_{PT23}$, avrPtoBH-F and avrPtoBH-R; for $avrPtoB_{B728a}$, B728a-F and B728a-R; and for *hopPmaL*, hopPmaL-F and hopPmaL-R. PCR products were cloned into pCR2.1 for sequencing, and the EcoRI fragments were subcloned into an EcoRI-digested pJG4-5 vector. The pJG4-5 constructs were introduced into a yeast strain containing pEG202::*Pto* and a reporter vector (10). Yeast cells containing both prey and bait proteins were streaked on medium containing galactose and 5-bromo-4-chloro-3-indolyl-β-D-galactopyranoside (X-Gal). Photographs were taken after 2 days of incubation of the plates at 30°C.

Construction of Δ*avrPto*Δ*avrPtoB* expressing *avrPtoB* homologs. DNA fragments containing the native *hrp* box and the open reading frames of individual *avrPtoB* homologs were PCR amplified using the primers listed in Table 2 and were cloned into pCR2.1 for sequencing. Primers avrPtoB-*hrp* and avrPtoBH-R were used to amplify $avrPtoB_{T1}$ and $avrPtoB_{PT23}$. $avrPtoB_{B728a}$ was amplified using primers B728a-*hrp* and B728a-R, and *hopPmaL* was amplified using primers hopPmaL-*hrp* and hopPmaL-R. The EcoRI fragments from pCR2.1 containing individual *avrPtoB* homologs were subcloned into the broad-host-range vector pCPP45 to create p$AvrPtoB_{T1}$, p$avrPtoB_{PT23}$, p$avrPtoB_{B728a}$, and p*hopPmaL*, and this was followed by introduction into Δ*avrPto*Δ*avrPtoB* using triparental mating to obtain Δ*avrPto*Δ*avrPtoB* expressing *avrPtoB* homologs under the control of an *hrp* promoter. Δ*avrPto*Δ*avrPtoB* strains containing an empty vector [referred to below as Δ*avrPto*Δ*avrPtoB*(ev)] and *avrPtoB* [referred to below as Δ*avrPto*Δ*avrPtoB* (*avrPtoB*)] were constructed in a previous study (26).

Plant assays. Tomato (*Solanum lycopersicon*) Rio-Grande (RG) lines were grown as previously described (23) and included four genotypes: RG-PtoR (*Pto*/*Pto*, *Prf*/*Prf*), RG-pto11 (*pto11*/*pto11*, *Prf*/*Prf*), RG-prf3 (*Pto*/*Pto*, *prf3*/*prf3*), and RG-PtoS, which is nearly isogenic with RG-PtoR (35). For pathogenicity assays, bacterial suspensions containing 1×10^4 CFU ml^{-1} in 10 mM $MgCl_2$ and 0.002% Silwet L-77 (Cromptom Co., Middlebury, CT) were vacuum infiltrated into leaves of 4-week-old plants. Disease development and bacterial populations were monitored every other day after inoculation. Bacteria recovered from plants were plated on KB medium containing rifampin. Numbers of specks were de-

termined for nine independent 1-cm^2 areas. Fully expanded leaflets were used for recovery of bacteria and counting of lesions.

Construction of strains for *Agrobacterium*-mediated transient assay. KpnI/XbaI fragments of the pCR2.1 constructs, which were generated previously for yeast two-hybrid interactions, were subcloned into a KpnI/XbaI-digested pBTEX binary vector. The pBTEX constructs were electroporated into *A. tumefaciens* GV2260, and the strains were used to syringe infiltrate leaves of 4-week-old tomato plants and 6-week-old *Nicotiana benthamiana* plants at a final OD_{600} of 0.1. *A. tumefaciens* strains carrying transgenes of *avrPto*, *avrPtoB*, or *Pto* were constructed in previous studies (1, 39). *Agrobacterium*-mediated transient assays were performed as described previously (37).

Ion leakage assays. Leaf disks excised from the areas infiltrated with *Agrobacterium* were incubated in water at room temperature for 3 h. Each solution was used to measure sample conductivity with an Acorn series CON5 m (OAKTON Instruments, Vernon Hills, IL). Leaf disks taken from areas where there was no infiltration with *Agrobacterium* were used as blank controls to normalize sample conductivity. Ion leakage was expressed as the difference in conductivity between the blank control and samples.

RESULTS

Sequence comparisons of *avrPtoB* homologs. Southern blot analysis revealed that many *Pseudomonas* spp. strains contain *avrPtoB* sequences (20, 24; data not shown). Among these, *P. syringae* pv. tomato strains T1, PT23, and JL1065, *P. syringae* pv. syringae B728a and *P. syringae* pv. maculicola ES4326 were chosen for cloning and characterization of their *avrPtoB* homologs. Previously, an AvrPtoB domain involved in recognition by Pto was mapped to amino acids 1 to 308 of AvrPtoB, and an anti-PCD domain was identified in the C terminus (1). Alignments obtained with ClustalW (40) revealed that these two domains are for the most part conserved among AvrPtoB and its homologs, although many amino acid substitutions and numerous insertions and deletions distinguish them, particularly in the region from amino acid 128 to amino acid 202 (Fig. 1A).

As reported previously, AvrPtoB exhibits 52% sequence similarity with VirPphA. Homologs of VirPphA were identified in *P. syringae* pv. phaseolicola 1448A, *P. syringae* pv. glycinea ($VirPphA_{Pgy}$; accession no. AJ439728), and *P. syringae* pv. savastanoi ($VirPphA_{Psv}$; accession no. AJ439729) (19). We performed phylogenetic and molecular evolutionary analyses of the AvrPtoB/VirPphA family (also known as the HopAB family) using MEGA, version 2.1 (25). These analyses showed that AvrPtoB homologs from *P. syringae* pv. tomato strains T1, PT23, and JL1065 are closely related to HopPmaL from *P. syringae* pv. maculicola ES4326 (Fig. 1B). The AvrPtoB homolog from *P. syringae* pv. syringae B728a is more similar to VirPphA from *P. syringae* pv. phaseolicola than to AvrPtoB. Based on a recently introduced nomenclature (27), the homologs that we cloned were derived from the HopAB1 and HopAB3 families (although note that HopPmaL is a truncated version of the other members of the HopAB3 family [Fig. 1A]). At present, AvrPtoB is the only member of the HopAB2 family. In order to highlight the many functional similarities of the new homologs to AvrPtoB (see below), we refer to them below as $avrPtoB_{T1}$, $avrPtoB_{PT23}$, $avrPtoB_{JL1065}$, and $avrPtoB_{B728a}$.

avrPtoB is 77% identical at the nucleotide level (66% identical at the amino acid level) to $avrPtoB_{T1}$, $avrPtoB_{PT23}$, and $avrPtoB_{JL1065}$. The nucleotide sequences of $avrPtoB_{PT23}$ and $avrPtoB_{JL1065}$ are identical, and each exhibits 99.7% identity to $avrPtoB_{T1}$. Because $AvrPtoB_{PT23}$ and $AvrPtoB_{JL1065}$ are identical, only $AvrPtoB_{PT23}$ was characterized further. All three homologs encode 579-amino-acid predicted proteins with molecular masses of 61.9 kDa. $AvrPtoB_{T1}$ differs from $AvrPtoB_{PT23}$ and $AvrPtoB_{JL1065}$ by only three amino acids, located at residues 35, 493, and 515. $avrPtoB_{B728a}$ exhibits 69% nucleotide identity (52% amino acid identity) with *avrPtoB* and encodes a 516-amino-acid predicted protein with a molecular mass of 57.6 kDa. *hopPmaL* encodes a shorter protein (385 amino acids) with a molecular mass of 42 kDa, and the HopPmaL protein is therefore similar to the C-terminal truncated form of AvrPtoB, AvrPtoBΔ6 (1, 11). In the region that overlaps with *avrPtoB*, *hopPmaL* exhibits 66.5% nucleotide identity (58% amino acid identity).

Expression of endogenous *avrPtoB* homologs in *P. syringae* strains. Based on previous observations, *P. syringae* pv. tomato strains containing an *avrPtoB* homolog would be expected to be avirulent on tomato plants expressing Pto. However, only *P. syringae* pv. tomato PT23 and *P. syringae* pv. tomato JL1065 are avirulent on Pto-expressing tomatoes, whereas *P. syringae* pv. tomato T1 and *P. syringae* pv. maculicola ES4326 are virulent (data not shown for *P. syringae* pv. maculicola ES4326). RT-PCR using gene-specific primers (Table 2) was performed to test whether the differences are due to lack of expression of the *avrPtoB*-related genes in T1 and ES4326. Abundant *hrp*-dependent accumulation of endogenous *avrPtoB*, $avrPtoB_{T1}$, $avrPtoB_{B728a}$, and *hopPmaL* transcripts was observed, whereas endogenous $avrPtoB_{PT23}$ and $avrPtoB_{JL1065}$ transcripts were present at much lower levels (Fig. 2). The lower transcript abundance in *P. syringae* pv. tomato PT23 and *P. syringae* pv. tomato JL1065 was not due to primer problems because the primer sets used for $avrPtoB_{T1}$, $avrPtoB_{PT23}$, and $avrPtoB_{JL1065}$ amplified these genes with similar efficiencies when genomic DNA was used as a template (data not shown). Therefore, the faint bands detected for *P. syringae* pv. tomato PT23 and *P. syringae* pv. tomato JL1065 likely indicate that their *avrPtoB* homologs are not expressed at high levels when these two strains are grown in *hrp*-inducing minimal medium (HrpMM).

All AvrPtoB proteins tested except $AvrPtoB_{T1}$ are produced and secreted in an *hrp*-dependent manner. The accumulation of a protein corresponding to AvrPtoB and its homologs was examined using anti-AvrPtoB antibodies. Production of endogenous AvrPtoB, $AvrPtoB_{PT23}$, $AvrPtoB_{JL1065}$, and HopPmaL proteins was detected in both bacterial cells and culture medium after growth in HrpMM, indicating that these four proteins accumulate and are secreted in an *hrp*-dependent manner apparently not correlated with transcript levels (Fig. 3A and B).

Surprisingly, no AvrPtoB-related proteins were detected in *P. syringae* pv. tomato T1 or *P. syringae* pv. syringae B728a. Although AvrPtoB and $AvrPtoB_{B728a}$ exhibit 52% amino acid sequence identity to each other, regions of similarity are dispersed throughout the proteins. Therefore, it is possible that our anti-AvrPtoB antibodies did not cross-react with $AvrPtoB_{B728a}$. Indeed, $AvrPtoB_{B728a}$ protein could be detected by using anti-HA antibody but not by using anti-AvrPtoB antibody when an HA-tagged version of $AvrPtoB_{B728a}$ was expressed in *P. syringae* pv. syringae B728a (data not shown). However, $AvrPtoB_{T1}$ differs by only three amino acids from $AvrPtoB_{PT23}$ and $AvrPtoB_{JL1065}$, and we detected both of the latter proteins using our anti-AvrPtoB antibodies. Thus, it is unlikely that the anti-AvrPtoB antibodies fail to cross-react with $AvrPtoB_{T1}$. To examine this observation further, a broad-host-range vector

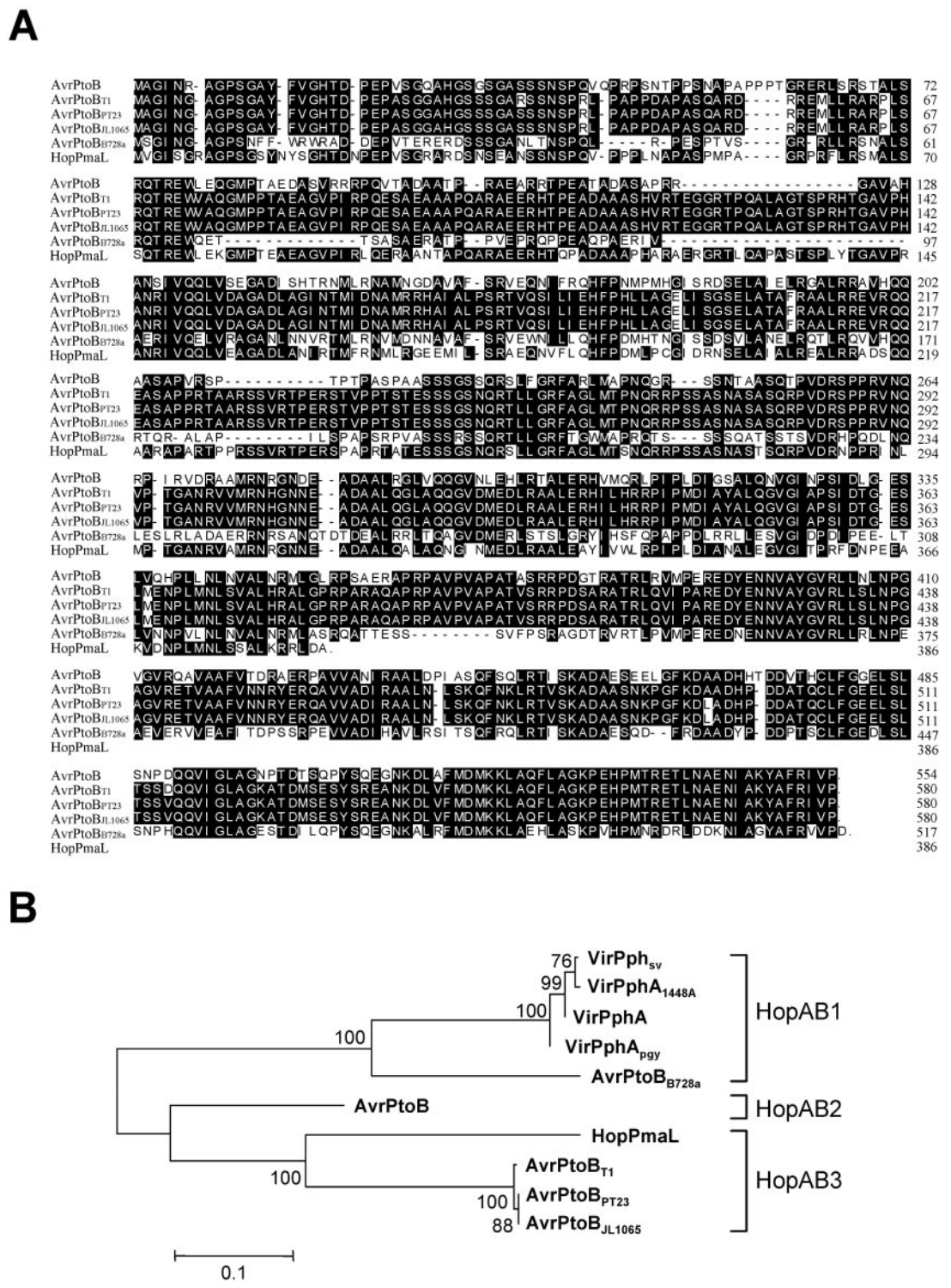

FIG. 1. Sequence comparisons for AvrPtoB and AvrPtoB homologs. (A) Alignment of the amino acid sequences of AvrPtoB and five AvrPtoB homologs. Alignment was performed using ClustalW (40). Conserved residues are highlighted. The domain required for Pto interaction in a yeast two-hybrid system encompasses AvrPtoB residues 1 to 308. The domain required for the anti-PCD function consists of AvrPtoB residues 309 to 553 (1). The GenBank accession numbers are DQ133533 (*avrPtoB$_{T1}$*), DQ133534 (*avrPtoB$_{PT23}$*), and DQ133535 (*avrPtoB$_{JL1065}$*). (B) Neighbor-joining tree for AvrPtoB and eight other members of the AvrPtoB/VirPphA (HopAB) family, which was constructed using MEGA, version 2.1 (25). The horizontal branch lengths are proportional to the estimated numbers of amino acid substitutions, and bootstrap scores (expressed as percentages) are indicated at the nodes.

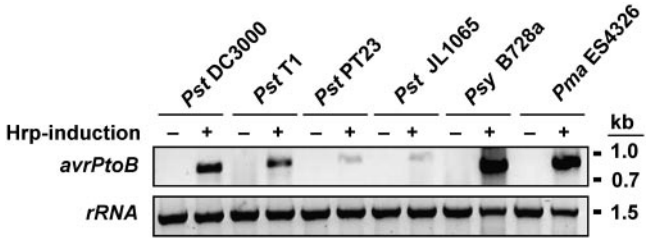

FIG. 2. RT-PCR analysis of *avrPtoB* homolog transcripts. Total RNA was isolated from each *Pseudomonas* strain after growth without (lanes −) or with (lanes +) Hrp induction. RT-PCR was performed as described in Materials and Methods using gene-specific primers; primers for 16S rRNA were used as an internal control. The PCR products were separated on an agarose gel and stained with ethidium bromide. Transcripts for each of the AvrPtoB homologs could be detected in the strain from which the corresponding gene was isolated.

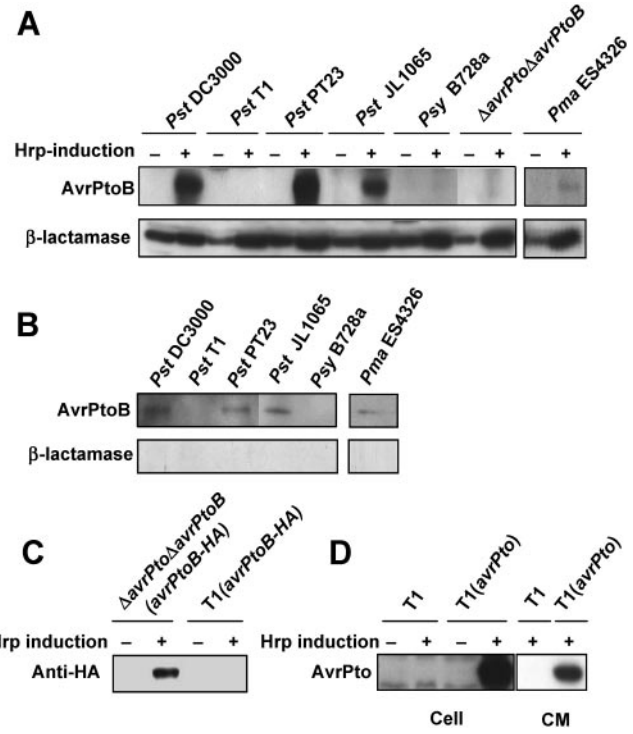

FIG. 3. Analysis of protein accumulation and secretion of AvrPtoB and AvrPtoB homologs. (A) AvrPtoB and AvrPtoB homolog proteins were detected in cells of *P. syringae* strains by Western blotting using anti-AvrPtoB antibodies (see Materials and Methods). β-Lactamase was included as a loading control. Strains were grown without (lanes −) or with (lanes +) Hrp induction. AvrPtoB or AvrPtoB homolog proteins were detected in *P. syringae* pv. tomato DC3000, *P. syringae* pv. tomato PT23, *P. syringae* pv. tomato JL1065, and *P. syringae* pv. maculicola ES4326. (B) Secretion of AvrPtoB and AvrPtoB homologs into the culture medium in an Hrp-dependent manner was analyzed by Western blotting using anti-AvrPtoB antibodies. Secretion of AvrPtoB proteins was observed for all strains except T1 and B728a (see Results). Strains were grown in Hrp-inducing conditions. β-Lactamase antibodies were used as a control, and, as expected, no β-lactamase was detected in the culture medium. (C) Analysis of AvrPtoB-HA protein accumulation in strains DC3000Δ*avrPto*Δ*avrPtoB* and T1 by Western blotting using anti-HA antibodies. An AvrPtoB-HA-expressing plasmid was transformed into the two strains, and the strains were grown without (lanes −) or with (lanes +) Hrp induction. AvrPtoB was observed to accumulate in DC3000Δ*avrPto*Δ*avrPtoB* but not in T1. (D) Analysis of accumulation and secretion of AvrPto in strain T1. T1 and a derivative expressing AvrPto from a plasmid were grown without (lanes −) or with (lanes +) Hrp induction. Extracts were prepared from cells or from the culture medium (CM). Western blotting with anti-AvrPto antibodies detected AvrPto in both total cells and the culture medium, indicating that, as expected, this protein is expressed by and secreted from strain T1.

expressing an HA-tagged version of AvrPtoB was introduced into Δ*avrPto*Δ*avrPtoB* and *P. syringae* pv. tomato T1, and Avr PtoB protein expression was examined using anti-HA antibodies. *hrp*-dependent expression of the AvrPtoB::HA protein was detected in Δ*avrPto*Δ*avrPtoB*(*avrPtoB*) but not in *P. syringae* pv. tomato *T1* expressing *avrPtoB*::*HA* (Fig. 3C). To test whether the type III secretion system (TTSS) is functional in *P. syringae* pv. tomato T1, *P. syringae* pv. tomato T1 carrying *avrPto* under control of its native promoter [referred to below as *P. syringae* pv. tomato T1(*avrPto*)] was used to perform the same translation/secretion assay used with the AvrPtoB proteins. In *P. syringae* pv. tomato T1(*avrPto*), AvrPto was detected in both bacterial cells and culture medium after induction of bacterial gene expression in HrpMM, indicating that the TTSS is functional in *P. syringae* pv. tomato T1 (Fig. 3D). Thus, we concluded that strain T1 appears to selectively interfere with accumulation of both $AvrPtoB_{T1}$ and AvrPtoB by an unknown mechanism.

AvrPtoB homologs interact with Pto in a yeast two-hybrid system and confer avirulence activity to Δ*avrPto*Δ*avrPtoB* in tomato leaves expressing Pto. AvrPtoB was originally isolated as a Pto-interacting protein from a yeast two-hybrid screening analysis. We found that like AvrPtoB, all of the AvrPtoB homologs interact with Pto in a yeast two-hybrid system (Fig. 4A). To examine the ability of each AvrPtoB protein to elicit Pto-mediated resistance, we relied on the *avrPto*/*avrPtoB* deletion mutant of *P. syringae* pv. tomato DC3000 (Table 1) (29). This mutant causes disease in tomato lines expressing Pto and has a reduced ability to produce specks on susceptible tomato plants (26). Introduction of AvrPtoB on a broad-host-range vector into the *avrPto*/*avrPtoB* mutant restored its ability to elicit Pto-mediated resistance and to produce specks similar to those produced by wild-type *P. syringae* pv. tomato DC3000. This mutant therefore was a useful tool to study the avirulence and virulence activities of *avrPtoB* homologs from different *Pseudomonas* strains.

To determine whether the interaction with Pto in the yeast two-hybrid system correlated with the avirulence activity of *avrPtoB* homologs in *Pseudomonas* spp., each gene was introduced on a broad-host-range plasmid into Δ*avrPto*Δ*avrPtoB* and tested for its ability to elicit resistance in tomato lines expressing Pto. Pto-dependent resistance was observed on leaves that were vacuum infiltrated with Δ*avrPto*Δ*avrPtoB* expressing *avrPtoB*, $avrPtoB_{T1}$, $avrPtoB_{PT23}$, $avrPtoB_{B728a}$, or *hopPmaL*, whereas disease developed on tomato leaves inoculated with control strain Δ*avrPto*Δ*avrPtoB*(ev) (Fig. 4B). The sizes of the bacterial populations were restricted to 10^4 to 10^5 CFU cm^{-2} in leaves infiltrated with Δ*avrPto*Δ*avrPtoB* expressing *avrPtoB* and each of the *avrPtoB* homologs (Fig. 4C). In contrast, bacteria grew to a level of 5×10^7 CFU cm^{-2} in leaves infiltrated with the control Δ*avrPto*Δ*avrPtoB*(ev) strain.

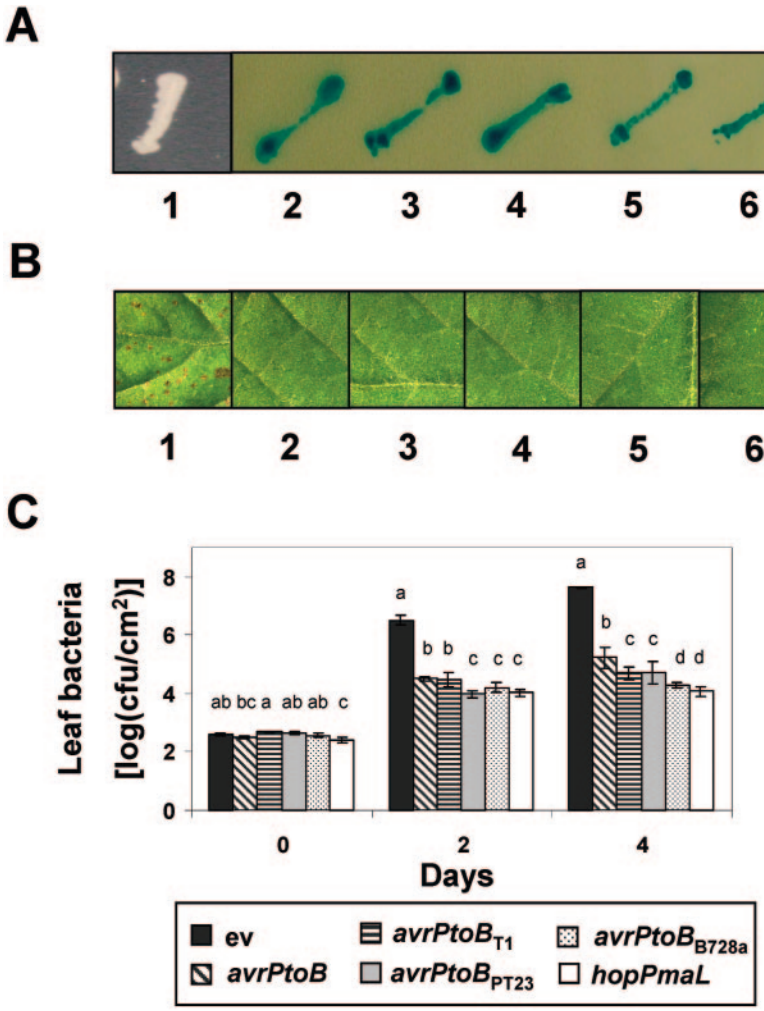

FIG. 4. AvrPtoB homologs interact with Pto and elicit Pto-dependent resistance. (A) Yeast two-hybrid interactions of Pto with AvrPto or the AvrPtoB homologs. Image 1, empty vector; image 2, AvrPtoB; image 3, $AvrPtoB_{T1}$; image 4, $AvrPtoB_{PT23}$; image 5, $AvrPtoB_{B728a}$; image 6, HopPmaL. (B) Elicitation of Pto-dependent resistance by infiltration of RG-PtoR leaves with 10^4 CFU ml^{-1} Δ*avrPto*Δ*avrPtoB* expressing the following genes: none (empty vector) (leaf 1), *avrPtoB* (leaf 2), $avrPtoB_{T1}$ (leaf 3), $avrPtoB_{PT23}$ (leaf 4), $avrPtoB_{B728a}$ (leaf 5), and *hopPmaL* (leaf 6). Photographs were taken 6 days after inoculation. Disease developed 3 days after inoculation of RG-PtoR leaves with only Δ*avrPto*Δ*avrPtoB*(ev) (leaf 1). (C) Bacterial populations in RG-PtoR tomato leaves at 0, 2, and 4 days after inoculation with DC3000Δ*avrPto*Δ*avrPtoB* expressing the genes indicated. Leaves were vacuum infiltrated with 10^4 CFU ml^{-1} of bacteria. The error bars indicate the standard deviations for three replicates. Data analysis was performed using Duncan's multiple-range test. Means with the same letter above the bars are not different at a significance level of 5%. The experiments were performed twice, and similar results were obtained.

Therefore, like *avrPtoB*, all of the *avrPtoB* homologs confer avirulence activity to Δ*avrPto*Δ*avrPtoB*.

***avrPtoB* homologs enhance lesion-forming ability and growth of Δ*avrPto*Δ*avrPtoB* in susceptible tomato leaves.** Susceptible tomato lines RG-PtoS, RG-pto11, and RG-prf3 (see Materials and Methods) were used for pathogenicity assays. Although some variability was associated with certain tomato lines and *avrPtoB* homologs, compared to leaves infiltrated with Δ*avrPto*Δ*avrPtoB*(ev), more specks were observed on tomato leaves inoculated with Δ*avrPto*Δ*avrPtoB* expressing *avrPtoB* or one of the homologs (Fig. 5). The only exception was the finding that *avrPtoB* did not restore the lesion-forming ability of Δ*avrPto*Δ*avrPtoB* when it was inoculated onto leaves of tomato line RG-pto11. These results indicate that each of the *avrPtoB* homologs promotes bacterial virulence, in part, by enhancing the development of disease symptoms.

To determine if the increased disease symptoms that we observed correlated with increased bacterial growth, we next measured populations of Δ*avrPto*Δ*avrPtoB* expressing *avrPtoB* or the *avrPtoB* homologs in leaves of each tomato genotype. At day 2, in tomato lines RG-PtoS and RG-prf3 Δ*avrPto*Δ*avrPtoB* expressing *avrPtoB* or *avrPtoB* homologs showed between 2- and 10-fold enhancement of bacterial growth compared to Δ*avrPto*Δ*avrPtoB*(ev) (Fig. 6A and B). However, the sizes of the populations of all strains were similar 4 days after inoculation. We reported similar observations previously for AvrPtoB (26) and hypothesized that the enhanced disease symptoms seen with the AvrPtoB-expressing strain, compared

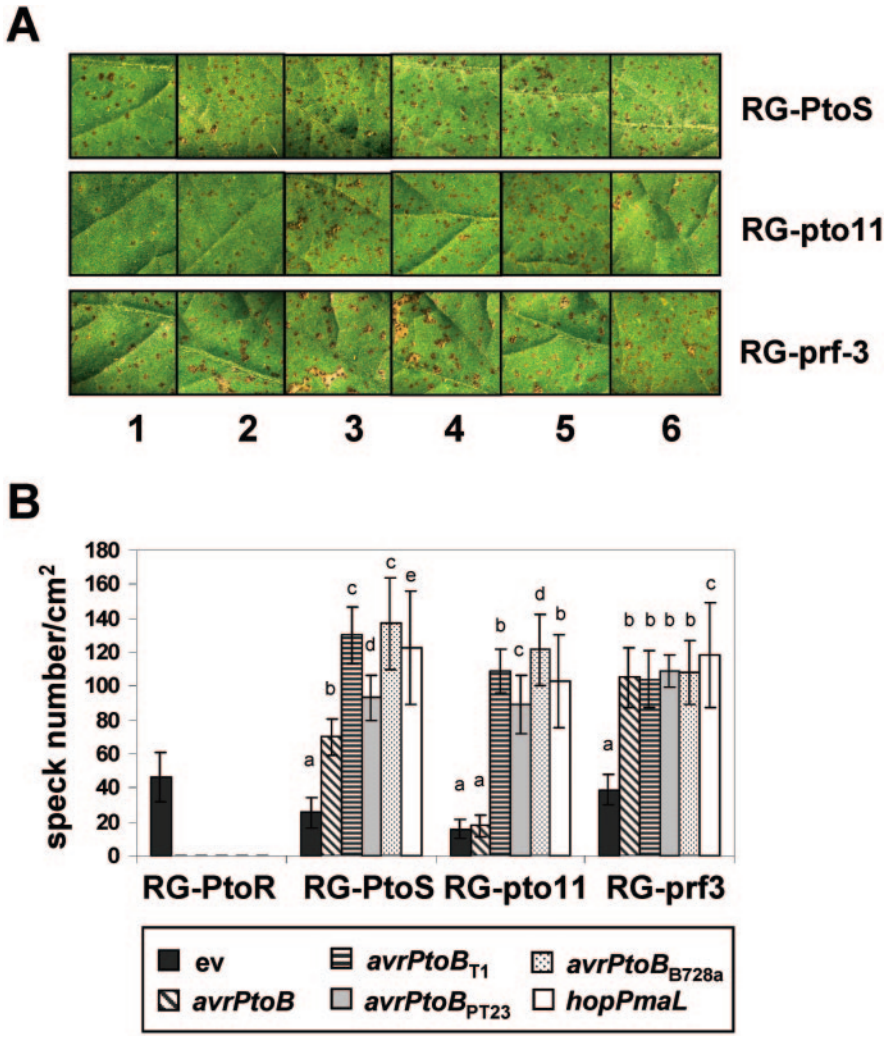

FIG. 5. Lesion-forming ability on susceptible tomato leaves of DC3000Δ*avrPto*Δ*avrPtoB* strains expressing AvrPtoB or the AvrPtoB homologs. (A) Host defense response or disease symptoms in RG-PtoS, RG-pto11, and RG-prf3 plants 6 days after inoculation with DC3000Δ*avrPto*Δ*avrPtoB* strains expressing the following genes: none (empty vector) (leaf 1), *avrPtoB* (leaf 2), $avrPtoB_{T1}$ (leaf 3), $avrPtoB_{PT23}$ (leaf 4), $avrPtoB_{B728a}$ (leaf 5), and *hopPmaL* (leaf 6). Photographs were taken under a dissecting microscope 6 days after inoculation, and each area shown is 1 cm^2. (B) Numbers of specks on tomato leaves inoculated with DC3000Δ*avrPto*Δ*avrPtoB* expressing the genes indicated. The numbers of specks per cm^2 were counted for nine independent areas of the leaflet, and the error bars indicate standard deviations. Leaflets at the same position of each plant were chosen for counting numbers of specks and photography. Means with the same letter above the bars are not different at a significance level of 5%. The experiments were performed twice, and similar results were obtained.

to the empty-vector control strain, were probably due to the faster growth of the former strain at early times.

In leaves of tomato line RG-pto11 2 days after inoculation, expression of each *avrPtoB* homolog promoted 5- to 10-fold more bacterial growth in Δ*avrPto*Δ*avrPtoB* than in either Δ*avrPto*Δ*avrPtoB*(ev) or Δ*avrPto*Δ*avrPtoB*(*avrPtoB*) (Fig. 6C). At day 4, the populations of Δ*avrPto*Δ*avrPtoB*(ev) and Δ*avrPto*Δ*avrPtoB*(*avrPtoB*) were still smaller than the populations of the strains expressing the *avrPtoB* homologs (Fig. 6C). The smaller populations of Δ*avrPto*Δ*avrPtoB*(ev) and Δ*avrPto*Δ*avrPtoB*(*avrPtoB*) correlated with the lower numbers of specks produced by these two strains on RG-pto11 (Fig. 5B).

$AvrPtoB_{T1}$, $AvrPtoB_{PT23}$, and $AvrPtoB_{B728a}$ inhibit PCD. AvrPtoB has the ability to suppress plant immunity by inhibiting PCD (1). The anti-PCD domain has been mapped to the C terminus of AvrPtoB, which exhibits 73% sequence identity with $AvrPtoB_{T1}$ and $AvrPtoB_{PT23}$ and 59% sequence identity with $AvrPtoB_{B728a}$. To determine if these three *avrPtoB* homologs have anti-PCD activity, *avrPto* and *Pto* were coexpressed with $avrPtoB_{T1}$, $avrPtoB_{PT23}$, or $avrPtoB_{B728a}$ using *Agrobacterium*-mediated transient expression in leaves of *N. benthamiana*. Three days after agroinfiltration, the cell death normally initiated by AvrPto and Pto was inhibited by coexpression of AvrPtoB. $AvrPtoB_{T1}$, $AvrPtoB_{PT23}$, or $AvrPtoB_{B728a}$ each inhibited cell death triggered by AvrPto/Pto (Fig. 7A). Ion leakage in the area infiltrated with *A. tumefaciens* was measured over a 7-day period to quantify host cell death. Each of the AvrPtoB homologs suppressed AvrPto/Pto-mediated ion leakage compared to the empty-vector control, and AvrPtoB showed the most stable suppression activity (Fig. 7B).

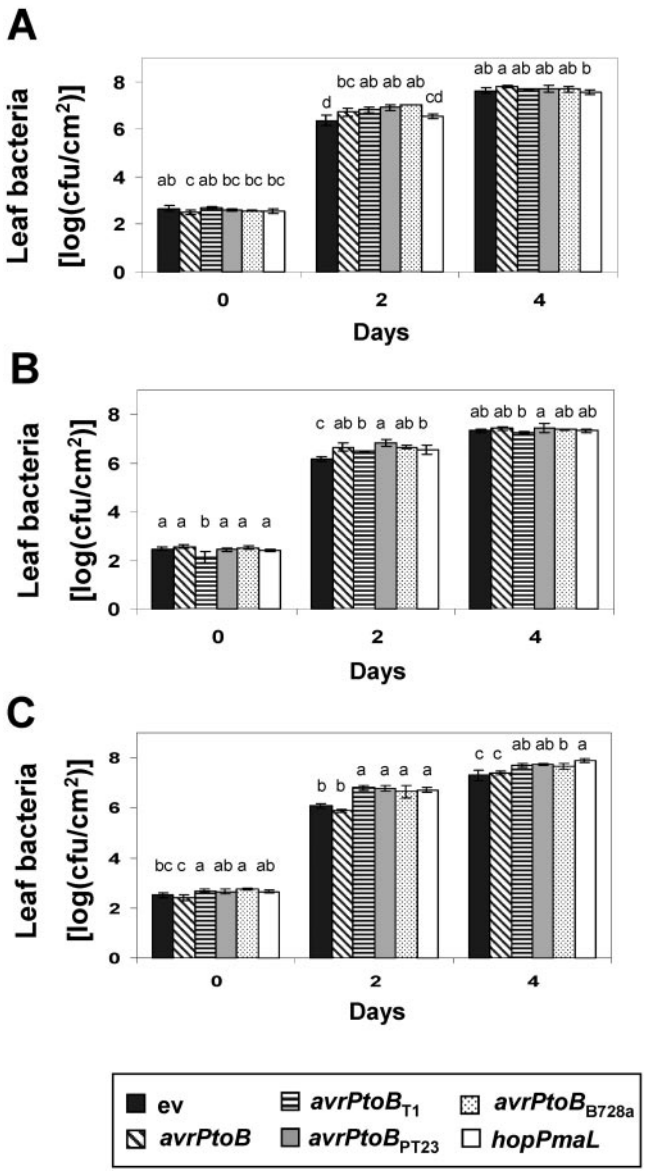

FIG. 6. Growth of DC3000Δ*avrPto*Δ*avrPtoB* expressing AvrPtoB or the AvrPtoB homologs. (A) RG-PtoS. (B) RG-prf3. (C) RG-pto11. The bacterial strains were vacuum infiltrated into leaves of Rio-Grande tomato lines, and the bacterial populations were measured 0, 2, and 4 days after inoculation. The error bars indicate the standard deviations for three 1-cm-diameter leaf disks. Data analysis was performed using Duncan's multiple-range test. Means with the same letter above the bars are not different at a significance level of 5%. ev, empty vector pCPP45. The experiments were performed twice, and similar results were obtained.

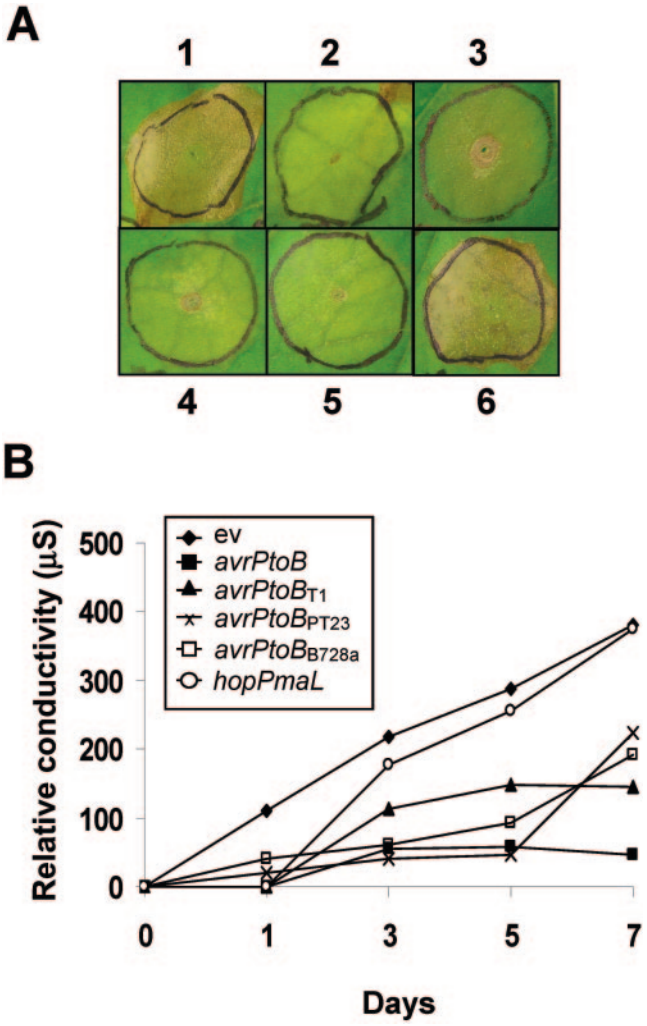

FIG. 7. Inhibition of programmed cell death by AvrPtoB in AvrPtoB homologs in *N. benthamiana* leaves. (A) The following proteins were coexpressed with AvrPto and Pto in mature leaves of *N. benthamiana* using *Agrobacterium*-mediated transient expression: none (empty vector) (leaf 1), AvrPtoB (leaf 2), AvrPtoB$_{T1}$ (leaf 3), AvrPtoB$_{PT23}$ (leaf 4), AvrPtoB$_{B728a}$ (leaf 5), and HopPmaL (leaf 6). Photographs were taken 7 days after *Agrobacterium* infiltration. (B) Ion leakage in the area infiltrated with *A. tumefaciens* expressing AvrPto, Pto, AvrPtoB, or AvrPtoB homologs 1, 3, 5, and 7 days after infiltration. Conductivity is indicated on the *y* axis.

Like AvrPtoBΔ6, a C terminus truncated form of AvrPtoB, HopPmaL triggered cell death in *N. benthamiana* when it was overexpressed in an *Agrobacterium*-mediated transient assay (data not shown). Lacking the anti-PCD domain, HopPmaL cannot inhibit cell death triggered by AvrPto/Pto (Fig. 7B).

DISCUSSION

The initial observation that AvrPtoB-related sequences are widely distributed among phytopathogenic bacteria suggested that members of this type III effector family might play an important role in bacterial virulence (23). Indeed, additional molecular studies have shown that AvrPtoB is a chimeric protein with distinct virulence activities in its N- and C-terminal domains (1). The C-terminal domain (amino acids 309 to 553) is sufficient for suppressing host programmed cell death elicited by Pto/AvrPto and a variety of other cell death inducers. Recent data suggest that the N-terminal domain (amino acids 1 to 308), which interacts with Pto, plays a role in promoting disease symptoms on susceptible plants (3; F. Xiao and G. B. Martin, unpublished data). Here we characterized representatives from each branch of the AvrPtoB/VirPphA (HopAB) family. These homologs have sequences that are divergent (52 to 65%) compared with the AvrPtoB sequence. Despite these differences, each of the AvrPtoB homologs interacts with Pto,

elicits Pto-dependent resistance when it is expressed in Δ*avrPto*Δ*avrPtoB*, and restores lesion-forming ability and enhances growth on susceptible tomato leaves when it is expressed in the Δ*avrPto*Δ*avrPtoB* mutant. Except for HopPmaL, which lacks the C-terminal domain, each of the AvrPtoB homologs suppresses PCD associated with immunity. These observations indicate that despite the fact that AvrPtoB homologs have undergone considerable evolution of their DNA sequences, key residues involved in virulence have been conserved among diverse AvrPtoB homologs. These homologs therefore should be useful tools in future studies to determine which residues play key roles in avirulence and virulence activities.

Our studies demonstrated that the *avrPtoB* homolog in *P. syringae* pv. maculicola ES4326, *hopPmaL*, is transcribed and translated and that the protein is secreted from bacterial cells in an *hrp*-dependent manner in vitro. Furthermore, HopPmaL both interacts with Pto in the yeast two-hybrid system and elicits Pto-specific resistance when it is delivered into tomato cells via Δ*avrPto*Δ*avrPtoB*. Nevertheless, *P. syringae* pv. maculicola ES4326 is fully virulent on Pto-expressing tomato leaves. We have not investigated the basis of this observation further, but one possible explanation for this discrepancy is that *P. syringae* pv. maculicola ES4326, like *P. syringae* pv. phaseolicola 1448a, from which VirPphA was first identified (18), might carry another effector which masks the avirulence activity of the AvrPtoB homolog.

We also observed that *P. syringae* pv. tomato T1, despite being virulent for Pto-expressing lines, also has an AvrPtoB homolog with an intact open reading frame. The $AvrPtoB_{T1}$ protein was functionally identical to AvrPtoB in terms of both its avirulence and virulence activities in our various assays (except for its activity on RG-pto11 [see below]). However, in contrast to *P. syringae* pv. maculicola ES4326, we were unable to detect the $AvrPtoB_{T1}$ protein in *P. syringae* pv. tomato T1, although the $avrPtoB_{T1}$ gene was transcribed. Notably, we found that AvrPtoB also did not accumulate in *P. syringae* pv. tomato T1 and that $AvrPtoB_{T1}$ is expressed normally in Δ*avrPto*Δ*avrPtoB*. Because transcription and translation are coupled in bacteria, this observation suggests that *P. syringae* pv. tomato T1 employs an unknown posttranslational mechanism to control the accumulation of AvrPtoB-like proteins. This mechanism appears to be specific because the AvrPto protein accumulated at normal levels in *P. syringae* pv. tomato T1 and was secreted in an *hrp*-dependent fashion.

Why are AvrPtoB-like proteins unable to accumulate in *P. syringae* pv. tomato T1? One possibility is that a helper protein of AvrPtoB (e.g., a chaperone), which is required for stabilization of the AvrPtoB protein or regulation of its translation or secretion, is missing in *P. syringae* pv. tomato T1. In certain bacterial pathogens of animals, storage of some virulence proteins and flagellar subunits before secretion involves association with specific chaperones (16). TTSS chaperones may function as (i) antiaggregation and stabilizing factors, (ii) signals for secretion and hierarchy-determining factors, (iii) antifolding factors, or iv) regulators of expression (9, 32). An additional role for chaperones as molecules that participate in coupling of translation to secretion was revealed for the anti-σ^{28} factor, FlgM, and its cognate chaperone, FlgN, in the flagellar system (22). Several chaperones in plant pathogens have been shown to interact with their cognate substrates and are required for secretion of their substrates into culture medium and translocation into plant cells. For example, $ShcF_{Pto}$ is known to stabilize its substrate ($HopF_{Pto}$) when it is expressed in *P. syringae* pv. phaseolicola (4, 21, 38, 42). Chaperone genes are typically located next to the gene encoding the chaperone substrate. However, no candidate chaperone genes have been found near *avrPtoB* coding sequences in DC3000. In addition, no obvious candidate helper proteins were identified in a yeast two-hybrid screening analysis for AvrPtoB-interacting proteins from DC3000 (A. S. Iyer and G. B. Martin, unpublished data). A second possibility to explain why AvrPtoB-like proteins do not accumulate in *P. syringae* pv. tomato T1 is that a specific negative regulator may function in *P. syringae* pv. tomato T1 to degrade $AvrPtoB_{T1}$ as soon as the protein is made. It has been demonstrated that a Lon protease in *P. syringae* pv. syringae 61, mediating degradation of HrpR, functions as a negative regulator of type III effectors. The Lon protein also mediates the proteolytic degradation of type III effectors to regulate the secretion of several effectors (5, 29). We are currently using different approaches to further dissect the mechanism underlying the regulation of AvrPtoB in *P. syringae* pv. tomato T1.

Although AvrPtoB and AvrPtoB homologs have similar avirulence and virulence activities, AvrPtoB had weaker effects on restricting bacterial growth on RG-PtoR, on promoting disease symptoms in susceptible tomato lines RG-PtoS and RG-pto11, and on enhancing bacterial growth in tomato line RG-pto11. Most notable was the inability of AvrPtoB, when expressed on a broad-host-range vector in Δ*avrPto*Δ*avrPtoB*, to enhance disease symptoms on leaves of RG-pto11 (Fig. 5B). *avrPtoB*, however, conferred increased virulence to Δ*avrPto*Δ*avrPtoB* in RG-PtoS and RG-prf3, indicating that *avrPtoB* is expressed and translocated at sufficient levels to alter pathogen growth in these plants. This observation suggests that the lack of enhanced growth in RG-pto11 is not the result of poor AvrPtoB translocation into the host. Rather, it might be due to recognition of AvrPtoB by the *Rsb* gene present in RG-pto11 (1).

The fact that many *Pseudomonas* pathovars encode AvrPtoB-like proteins with diverse C-terminal domains that nevertheless suppress host PCD highlights the importance of this virulence strategy. Inhibition of resistance gene-mediated responses may be one of the most common virulence functions of type III effectors. This phenomenon was demonstrated in *P. syringae* pv. phaseolicola 1448a race 6, in which both VirPphA and AvrPphC were found to suppress gene-for-gene resistance elicited by other effector proteins (18, 41). Later, AvrPtoB was shown to act generally as a cell death suppressor (1). More recent studies of type III effectors of DC3000 revealed that at least six effectors can suppress host PCD, strengthening the hypothesis that suppression of plant immunity is a general virulence mechanism utilized by type III effectors (3, 6, 8, 20, 28). In the future, it will be important to understand the molecular mechanisms underlying AvrPtoB suppression of PCD to gain further insight into its role in disease development.

The results reported here and in the previous study of *virPphA* and its homologs provide compelling evidence that broadly distributed type III effectors play important roles in bacterial pathogenesis. Further study of AvrPtoB homologs in their source bacterial strains should lead to insights into the

molecular basis of this virulence activity and why this activity is so important to pathogen fitness.

ACKNOWLEDGMENTS

We thank Alan Collmer for the kind gifts of pCPP2318 and anti-β-lactamase antibody. We acknowledge Hye-sook Oh for her assistance with the secretion assay and Olga del Pozo for her help with the ion leakage assay.

This work was supported by NSF grant DBI-0077622 (to G.B.M.) and by a government scholarship from the Ministry of Education, Taiwan, Republic of China (to N.-C.L.).

REFERENCES

1. **Abramovitch, R. B., Y.-J. Kim, S. Chen, M. B. Dickman, and G. B. Martin.** 2003. *Pseudomonas* type III effector AvrPtoB induces plant disease susceptibility by inhibition of host programmed cell death. EMBO J. **22:**60–69.
2. **Abramovitch, R. B., and G. B. Martin.** 2005. AvrPtoB: a bacterial type III effector that both elicits and suppresses programmed cell death associated with plant immunity. FEMS Microbiol. Lett. **245:**1–8.
3. **Abramovitch, R. B., and G. B. Martin.** 2004. Strategies used by bacterial pathogens to suppress plant defense. Curr. Opin. Plant Biol. **7:**356–364.
4. **Badel, J. L., K. Nomura, S. Bandyopadhyay, R. Shimizu, A. Collmer, and S. Y. He.** 2003. *Pseudomonas syringae* pv. *tomato* DC3000 HopPtoM (CEL ORF3) is important for lesion formation but not growth in tomato and is secreted and translocated by the Hrp type III secretion system in a chaperone-dependent manner. Mol. Microbiol. **49:**1239–1251.
5. **Bretz, J., L. Losada, K. Lisboa, and S. W. Hutcheson.** 2002. Lon protease functions as a negative regulator of type III protein secretion in *Pseudomonas syringae*. Mol. Microbiol. **45:**397–409.
6. **Bretz, J. R., N. M. Mock, J. C. Charity, S. Zeyad, C. J. Baker, and S. W. Hutcheson.** 2003. A translocated protein tyrosine phosphatase of *Pseudomonas syringae* pv. *tomato* DC3000 modulates plant defence response to infection. Mol. Microbiol. **49:**389–400.

6a. **Charlowski, A. O., H.-C. Huang, and A. Collmer.** 1997. Altered localization of HrpZ in *Pseudomonas syringae* pv. syringae *hrp* mutants suggests that different components of the type III secretion pathway control protein translocation across the inner and outer membranes of gram-negative bacteria. J. Bacteriol. **179:**3866–3874.

7. **Cohn, J. R., and G. B. Martin.** 2005. *Pseudomonas syringae* pv. *tomato* type III effectors AvrPto and AvrPtoB promote ethylene-dependent cell death in tomato. Plant J. **44:**139–154.
8. **Espinosa, A., M. Guo, V. C. Tam, Z. Q. Fu, and J. R. Alfano.** 2003. The *Pseudomonas syringae* type III-secreted protein HopPtoD2 possesses protein tyrosine phosphatase activity and suppresses programmed cell death in plants. Mol. Microbiol. **49:**377–387.
9. **Feldman, M. F., and G. R. Cornelis.** 2003. The multitalented type III chaperones: all you can do with 15 kDa. FEMS Microbiol. Lett. **219:**151–158.
10. **Golemis, E., J. Gyuris, and R. Brent.** 1996. Interaction trap/two-hybrid system to identify interacting protein, p. 20.1.1–20.1.28. *In* F. M. Ausubel, R. Brent, R. E. Kingston, D. D. Moore, J. G. Seidman, J. A. Smith, and K. Struhl (ed.), Current protocols in molecular biology. John Wiley & Sons Inc., New York, N.Y.
11. **Guttman, D. S., B. A. Vinatzer, S. F. Sarkar, M. V. Ranall, G. Kettler, and J. T. Greenberg.** 2002. A functional screen for the type III (Hrp) secretome of the plant pathogen *Pseudomonas syringae*. Science **295:**1722–1726.
12. **Ham, J. H., D. W. Bauer, D. E. Fouts, and A. Collmer.** 1998. A cloned *Erwinia chrysanthemi* Hrp (type III protein secretion) system functions in *Escherichia coli* to deliver *Pseudomonas syringae* Avr signals to plant cells and to secrete Avr proteins in culture. Proc. Natl. Acad. Sci. USA **95:**10206–10211.
13. **Hanahan, D.** 1985. Techniques for transformation of *E. coli*, p. 109–135. *In* D. M. Glover (ed.), DNA cloning: a practical approach. IRL Press, Oxford, United Kingdom.
14. **Harper, S., and D. W. Speicher.** 1997. Expression and purification of GST fusion proteins, p. 6.6.1–6.6.21. *In* J. E. Coligan, B. M. Dunn, D. W. Speicher, P. T. Wingfield, and H. L. Ploegh (ed.), Current protocols in protein science. John Wiley & Sons, Inc., New York, N.Y.
15. **Hauck, P., R. Thilmony, and S. Y. He.** 2003. A *Pseudomonas syringae* type III effector suppresses cell wall-based extracellular defense in susceptible *Arabidopsis* plants. Proc. Natl. Acad. Sci. USA **100:**8577–8582.
16. **He, S. Y., K. Nomura, and T. S. Whittam.** 2004. Type III protein secretion mechanism in mammalian and plant pathogens. Biochim. Biophys. Acta **1694:**181–206.
17. **Huynh, T. V., D. Dahlbeck, and B. J. Staskawicz.** 1989. Bacterial blight of soybean: regulation of a pathogen gene determining host cultivar specificity. Science **245:**1374–1377.
18. **Jackson, R. W., E. Athanassopoulos, G. Tsiamis, J. W. Mansfield, A. Sesma, D. L. Arnold, M. J. Gibbon, J. Murillo, J. D. Taylor, and A. Vivian.** 1999. Identification of a pathogenicity island, which contains genes for virulence and avirulence, on a large native plasmid in the bean pathogen *Pseudomonas syringae* pathovar phaseolicola. Proc. Natl. Acad. Sci. USA **96:**10875–10880.
19. **Jackson, R. W., J. W. Mansfield, H. Ammouneh, L. C. Dutton, B. Wharton, A. Ortiz-Barredo, D. L. Arnold, G. Tsiamis, A. Sesma, D. Butcher, J. Boch, Y.-J. Kim, G. B. Martin, S. Tegli, J. Murillo, and A. Vivian.** 2002. Location and activity of members of a family of *virPphA* homologues in pathovars of *Pseudomonas syringae* and *P. savastanoi*. Mol. Plant Pathol. **3:**205–216.
20. **Jamir, Y., M. Guo, H. S. Oh, T. Petnicki-Ocwieja, S. Chen, X. Tang, M. B. Dickman, A. Collmer, and, J. R. Alfano** 2004. Identification of *Pseudomonas syringae* type III effectors that can suppress programmed cell death in plants and yeast. Plant J. **37:**554–565.
21. **Kabisch, U., A. Landgraf, J. Krause, U. Bonas, and J. Boch.** 2005. Type III secretion chaperones ShcS1 and ShcO1 from *Pseudomonas syringae* pv. *tomato* DC3000 bind more than one effector. Microbiology **151:**269–280.
22. **Karlinsey, J. E., J. Lonner, K. L. Brown, and K. T. Hughes.** 2000. Translation/secretion coupling by type III secretion systems. Cell **102:**487–497.
23. **Kim, Y.-J., N.-C. Lin, and G. B. Martin.** 2002. Two distinct *Pseudomonas* effector proteins interact with the Pto kinase and activate plant immunity. Cell **109:**589–598.
24. **King, E., M. Ward, and D. Raney.** 1954. Two simple media for the demonstration of pyocyanin and fluorescin. J. Lab. Clin. Med. **44:**301–307.
25. **Kumar, S., K. Tamura, I. B. Jakobsen, and M. Nei.** 2001. MEGA2: molecular evolutionary genetics analysis software. Bioinformatics **17:**1244–1245.
26. **Lin, N.-C., and G. B. Martin.** 2005. An *avrPto*/*avrPtoB* mutant of *Pseudomonas syringae* pv. *tomato* DC3000 does not elicit Pto-mediated resistance and is less virulent on tomato. Mol. Plant-Microbe Interact. **18:**43–51.
27. **Lindeberg, M., J. Stavrinides, J. H. Chang, J. R. Alfano, A. Collmer, J. L. Dangl, J. T. Greenberg, J. W. Mansfield, and D. S. Guttman.** 2005. Proposed guidelines for a unified nomenclature and phylogenetic analysis of type III Hop effector proteins in the plant pathogen *Pseudomonas syringae*. Mol. Plant-Microbe Interact. **18:**275–282.
28. **Lopez-Solanilla, E., P. A. Bronstein, A. R. Schneider, and A. Collmer.** 2004. HopPtoN is a *Pseudomonas syringae* Hrp (type III secretion system) cysteine protease effector that suppresses pathogen-induced necrosis associated with both compatible and incompatible plant interactions. Mol. Microbiol. **54:**353–365.
29. **Losada, L. C., and S. W. Hutcheson.** 2005. Type III secretion chaperones of *Pseudomonas syringae* protect effectors from Lon-associated degradation. Mol. Microbiol. **55:**941–953.
30. **McBride, K. E., and K. R. Summerfelt.** 1990. Improved binary vectors for *Agrobacterium*-mediated plant transformation. Plant Mol. Biol. **14:**269–276.
31. **Olmsted, J. B.** 1981. Affinity purification of antibodies from diazotized paper blots of heterogeneous protein samples. J. Biol. Chem. **256:**11955–11957.
32. **Page, A. L., and C. Parsot.** 2002. Chaperones of the type III secretion pathway: jacks of all trades. Mol. Microbiol. **46:**1–11.
33. **Pedley, K. F., and G. B. Martin.** 2003. Molecular basis of Pto-mediated resistance to bacterial speck disease in tomato. Annu. Rev. Phytopathol. **41:**215–243.
34. **Ronald, P. C., J. M. Salmerson, F. Carland, M., and B. J. Staskawicz.** 1992. The cloned avirulence gene *avrPto* induces disease resistance in tomato cultivars containing the *Pto* resistance gene. J. Bacteriol. **174:**1604–1611.
35. **Salmeron, J. M., S. J. Barker, F. M. Carland, A. Y. Mehta, and B. J. Staskawicz.** 1994. Tomato mutants altered in bacterial disease resistance provide evidence for a new locus controlling pathogen recognition. Plant Cell **6:**511–520.
36. **Sambrook, J., E. F. Fritsch, and T. Maniatis.** 1989. Molecular cloning: a laboratory manual, 2nd ed. Cold Spring Harbor Laboratory Press, Cold Spring Harbor, N.Y.
37. **Sessa, G., M. D'Ascenzo, and G. B. Martin.** 2000. Thr38 and Ser198 are Pto autophosphorylation sites required for the AvrPto-Pto-mediated hypersensitive response. EMBO J. **19:**2257–2269.
38. **Shan, L., H. S. Oh, J. Chen, M. Guo, J. Zhou, J. R. Alfano, A. Collmer, X. Jia, and X. Tang.** 2004. The HopPtoF locus of *Pseudomonas syringae* pv. *tomato* DC3000 encodes a type III chaperone and a cognate effector. Mol. Plant-Microbe Interact. **17:**447–455.
39. **Tang, X., R. D. Frederick, J. Zhou, D. A. Halterman, Y. Jia, and G. B. Martin.** 1996. Initiation of plant disease resistance by physical interaction of AvrPto and Pto kinase. Science **274:**2060–2063.
40. **Thompson, J. D., D. G. Higgins, and T. J. Gibson.** 1994. CLUSTAL W: improving the sensitivity of progressive multiple sequence alignment through sequence weighting, position-specific gap penalties and weight matrix choice. Nucleic Acids Res. **22:**4673–4680.
41. **Tsiamis, G., J. W. Mansfield, R. Hockenhull, R. W. Jackson, A. Sesma, E. Athanassopoulos, M. A. Bennett, C. Stevens, A. Vivian, J. D. Taylor, and J. Murillo.** 2000. Cultivar-specific avirulence and virulence functions assigned to *avrPphF* in *Pseudomonas syringae* pv. *phaseolicola*, the cause of bean halo-blight disease. EMBO J. **19:**3204–3214.
42. **van Dijk, K., V. C. Tam, A. R. Records, T. Petnicki-Ocwieja, and J. R. Alfano.** 2002. The ShcA protein is a molecular chaperone that assists in the secretion of the HopPsyA effector from the type III (Hrp) protein secretion system of *Pseudomonas syringae*. Mol. Microbiol. **44:**1469–1481.